Strong mode coupling, bistable lasing, and switching mode dynamics in twin coupled microcavities

S. V. Zhukovsky[1], D. N. Chigrin[1], A. V. Lavrinenko[2], J. Kroha[1]

[1] Physikalisches Institut, Universität Bonn, Nussallee 12, D-53115 Bonn, Germany
[2] COM-DTU, Department of Communication, Optics and Materials, NanoDTU, Technical University of Denmark, Building 345V, DK-2800 Kgs. Lyngby, Denmark

ABSTRACT

Bistable lasing in twin coupled microcavities is demonstrated analytically and numerically, underlying a new principle of a multiple-wavelength microlaser where the lasing wavelength is switched by locking into the desired mode in a multimode resonator. The bistability appears due to an interplay between coherent and incoherent mode interaction processes, assisted by similarity between the spatial intensity distribution of the modes in the gain region. The wavelength switching dynamics in a model system of twin defects in a photonic crystal is explained on the basis of the theoretical analysis presented.

1. INTRODUCTION

Micro- and nanostructure based photonic devices play a key part in many areas of optoelectronics, integrated optics, and optical telecommunications. Of these devices, microlasers[1,2] provide an important milestone, facilitating low-threshold,[3,4] integrated, on-chip coherent light sources, which can also be utilized for quantum computing and cavity quantum electrodynamics studies. Making microlasers capable of multiple-wavelength operation has the obvious advantage in providing an additional degree of freedom in on-chip light control. However, the small cavity size makes it increasingly difficult to introduce a tuning element into the laser resonator. Instead, a tunable microlaser is commonly envisaged as a system where the entire single-mode cavity is subject to a modification by an external process, the most common among them being thermal, electro-optical, or micromechanical tuning mechanisms.[5–7]

Aside from the difficulties associated with the need to use external (and often quite slow) means to manipulate optical circuits, it is also non-trivial to make the cavity in question support single-mode lasing. This two-step process of first having to suppress multiple-mode operation and then devising a tuning mechanism for the cavity naturally calls forth an alternative principle: to start with a multimode resonator and then to lock it into one of its modes on demand, thereby creating a *switchable* (as opposed to tunable) microscopic laser light source. Since the mode locking is widely known to occur in lasers,[8] such switchable lasing provides a viable, potentially all-optical alternative to conventional microcavity tuning.

There are two problems to be seen on the way to switchable lasing. First, one does not want the locking signal to be monochromatic Instead, one can use a pulsed locking signal with the spectrum spanning all the modes in question, making the resonator lock to the signal's symmetry rather than its frequency. This idea was put forth earlier for coupled dielectric nanopillar waveguides[22] and successfully extended to the lasing regime in our recent investigations.[9]

A more serious and more fundamental problem lies in the nature of mode competition processes. When several modes interact in a cavity, those with a higher Q-factor tend to win the competition and dominate in lasing; if no mode becomes dominant, multimode lasing ensues.[8] On the contrary, switchable lasing implies that the resonator can have stable, single-mode lasing for more than one mode. In other words, the laser system in question must be *bi-* or *multistable*.

Theoretically, three lasing regimes of two-mode competition exist:[8,10] (i) domination of the mode with the significantly higher Q-factor; (ii) simultaneous two-mode lasing if the modes are close in Q and weakly coupled to each other; and (iii) bistable lasing when the coupling between the modes is strong. However, despite being a theoretically valid lasing regime, bistability means that cross-saturation between the modes exceeds their self-saturation, i.e., each mode saturates its counterpart more readily than it saturates itself. This can be imagined with relative ease in a system of two high-gain, low-Q coupled lasers[11,12] where the radiation coming out of each laser cavity is directed into the other cavity, and the

cavity finesse as well as feedback are specially weakened so to prevent formation of a compound dual-laser resonator.[13] In a microlaser where both modes coexist in the same cavity the incoherent mode coupling involving the spatial hole burning effects cannot be made that strong except by resorting to additional effects such as saturable absorbers or carrier diffusion,[14] or else to special cases such as counterpropagating modes in ring lasers or different polarizations in bistable laser diodes where the two modes (and two only) are degenerate so that the wavelength of both is the same.

In contrast, the present paper focuses on demonstration of bistable lasing with wavelength switching in coupled cavity based microlasers. The strong coupling between modes is achieved by coherent (presumably, population pulsation based) mode interaction processes. Contrary to the recent experimental results on bistable lasing in twin coupled microdisks[15] or microrings,[16] identical coupled cavities are considered, and a pulsed locking signal is used to switch the operating wavelength. Instead of being eigenmodes of slightly different cavities,[15,16] the modes in question are supermodes formed when identical single-mode cavities are coupled. The two-mode system based on twin defects in a 2D photonic crystal (PhC) lattice proposed in our recent work,[17] predicted to be capable of 20 nm wavelength switching on a sub-nanosecond time scale, has been analyzed in detail. The principle described readily allows extension to the coupled cavity based systems featuring more modes, as verified elsewhere[9] for nanopillar waveguides.

The structure of the paper is as follows. In Sec. 2 a coupled-mode multiscale analysis is developed for the eigenmodes of twin coupled microcavities. Starting from the Maxwell-Bloch semiclassical equations, the evolution of the modes and population inversion is derived. In Sec. 3 the resulting equations are analyzed. Bistable lasing regime has been obtained, and coherent mode interaction processes are singled out as the most probable cause. In Sec. 4 we investigate the dynamics of the mode-to-mode switching[17] using the models obtained in earlier sections. Finally, Sec. 5 summarizes the paper.

2. COUPLED TWO-MODE EQUATIONS

The small cavity size of microlasers causes their mode structure to show a greater variety compared to bulk cavities. In order to investigate the effects related to the mode structure, interaction, and dynamics of laser radiation in microstructures, one can use methods based on the eigenmode decomposition of the cavity field, similar to those developed for bulk resonators.[18,19] In this section, we extend the formalism developed in the work of S. Hodges *et al.*[18] to the case of two modes in a defect-based microcavity. Unlike most accounts, we derive the equations for laser dynamics without any specific assumptions for the mode geometry and simplify them for the case corresponding most closely to the eigenmodes of twin coupled cavities, i.e., the modes as similar to each other as possible, but still not identical in frequency.

2.1. Slowly varying envelope equations and two-mode temporal multiscale expansion

The system of basic equations is constructed of three parts: (i) the laser rate equations, reduced to the equation for population inversion of the laser transition; (ii) the equation of motion for macroscopic polarization density, obtained in a modified electronic oscillator model, and (iii) the scalar wave equation derived from the Maxwell equations for TM polarization in the 2D case. Applying the slowly varying envelope approximation,[8] the equations take the form[18]

$$\begin{aligned}
\frac{\partial}{\partial t}P(\mathbf{r},t) &= -\left(\gamma_\perp + \mathrm{i}\delta\right)P(\mathbf{r},t) - \frac{\mathrm{i}\mu^2}{\hbar}W(\mathbf{r},t)E(\mathbf{r},t), \\
\frac{\partial}{\partial t}W(\mathbf{r},t) &= \gamma_\parallel\left[R - W(\mathbf{r},t)\right] + \frac{\mathrm{i}}{4\hbar}\left[E(\mathbf{r},t)P^*(\mathbf{r},t) - E^*(\mathbf{r},t)P(\mathbf{r},t)\right], \\
\frac{1}{\epsilon_0}\frac{\partial^2}{\partial t^2}P(\mathbf{r},t)\mathrm{e}^{-\mathrm{i}\omega t} &= \left[c^2\nabla^2 - \epsilon(\mathbf{r})\frac{\partial^2}{\partial t^2} - \kappa(\mathbf{r})\frac{\partial}{\partial t}\right]E(\mathbf{r},t)\mathrm{e}^{-\mathrm{i}\omega t}.
\end{aligned} \tag{1}$$

Here $W(\mathbf{r},t)$ has the meaning of population inversion, R is the pumping rate, μ is the dipole moment, and the radiative and non-radiative decay rates are given by $\gamma_\perp$ and $\gamma_\parallel$, respectively. We consider a resonant system that features two eigenmodes with decay rates $\kappa_{1,2}$ and frequencies $\omega_{1,2} \equiv \omega_0 \mp \Delta\omega$ with the central frequency ω_0 shifted with respect to the lasing transition frequency ω_a by $\delta = \omega_a - \omega_0$ ($\Delta\omega, \delta \ll \omega_0$). We assume that the eigenmodes have the spatial structure given by $u_{1,2}(\mathbf{r})$. One can thus decompose the electric field $E(\mathbf{r},t)$ into spatially dependent mode profiles $u_{1,2}(\mathbf{r})$ multiplied by time dependent slowly varying envelope functions $E_{1,2}(t)$ as

$$E(\mathbf{r},t) = u_1(\mathbf{r})E_1(t)\mathrm{e}^{\mathrm{i}\Delta\omega t} + u_2(\mathbf{r})E_2(t)\mathrm{e}^{-\mathrm{i}\Delta\omega t} \equiv u_1(\mathbf{r})E_1(t)\mathrm{e}^{\phi_+} + u_2(\mathbf{r})E_2(t)\mathrm{e}^{\phi_-}. \tag{2}$$

Here and further, $\phi_\pm \equiv \pm \mathrm{i}\Delta\omega t$. Eq. (2) implies the use of the rotating wave approximation. Unlike the electric field, the polarization amplitudes $P_{1,2}(t)$ introduced likewise are not necessarily slowly varying and require further multiscale decomposition,[18,20] which in the case of two modes becomes

$$P(\mathbf{r},t) = u_1(\mathbf{r})\left[P_1^1(t) + P_1^2(t)\mathrm{e}^{2\phi_-}\right]\mathrm{e}^{\phi_+} + u_2(\mathbf{r})\left[P_2^1(t)\mathrm{e}^{2\phi_+} + P_2^2(t)\right]\mathrm{e}^{\phi_-}. \tag{3}$$

Finally, the population inversion $W(\mathbf{r},t)$ can only be decomposed in a temporal series at this stage:

$$W(\mathbf{r},t) = W^1(\mathbf{r},t)\mathrm{e}^{\phi_+} + W^2(\mathbf{r},t)\mathrm{e}^{\phi_-}. \tag{4}$$

The modes $u_j(\mathbf{r})$ are the solutions of the homogeneous wave equation assumed to form an orthonormal set in the cavity

$$\left[c^2\nabla^2 - \epsilon(\mathbf{r})\omega_j^2\right]u_j(\mathbf{r}) = 0, \qquad \int_C \mathrm{d}^3\mathbf{r}\epsilon(\mathbf{r})u_i^*(\mathbf{r})u_j(\mathbf{r}) = \delta_{ij}. \tag{5}$$

One can substitute Eqs. (2) and (3) into the equation for the electric field $E(\mathbf{r},t)$ in (1) with subsequent elimination of the spatial derivatives using Eq. (5). To disentangle the equations for each mode E_j, one typically applies the integration $\int \mathrm{d}^3\mathbf{r}u_j^*$ to both sides, using the normalization condition in (5) and the assumption that all time dependencies are slow enough. However, when the polarization term is present, this decoupling remains rigorously possible only as long as Eq. (5) remains true both with and without $\epsilon(\mathbf{r})$ in the integrand. This is automatically true only if ϵ is constant (the bulk-cavity case[18]). It remains approximately true if the majority of the modes' energy, as well as the laser active medium, are primarily located in a material with the same dielectric constant. This is often the case in microcavities. A more complicated case of distributed feedback structures requires both spectral and spatial multiscale analysis. (Such treatment was developed for PhC lasers,[20] the single-mode case investigated in detail.) Provided the decoupling can be made, one can further substitute Eqs. (2)–(4) into the system (1) and obtain the system of equations for P_j^q in terms of mode overlap integrals α_{ij}^{mn} and overlaps between the modes and the population inversion components W_{ij}^q:

$$\alpha_{ij}^{mn} \equiv \epsilon\int_G \mathrm{d}^3\mathbf{r}\, u_i^*(\mathbf{r})u_j(\mathbf{r})u_m^*(\mathbf{r})u_n(\mathbf{r}), \qquad W_{ij}^q(t) \equiv \epsilon\int_G \mathrm{d}^3\mathbf{r}\, u_i^*(\mathbf{r})W^q(\mathbf{r},t)u_j(\mathbf{r}). \tag{6}$$

The integration in Eqs. (6) is performed over the gain medium where $\epsilon(\mathbf{r})$ is assumed to be constant. The shape of the gain region itself can be arbitrary and does not have to be contiguous. The resulting equations for two modes, coupling two mode envelopes E_j, four polarization components P_j^q, and eight population inversion projections W_{ij}^q, have the form

$$\frac{\mathrm{d}}{\mathrm{d}t}E_j = -\frac{\kappa_j E_j}{2} + \frac{\mathrm{i}}{2\epsilon_0}\omega_j P_j^j, \tag{7}$$

$$\frac{\mathrm{d}}{\mathrm{d}t}P_j^{q=1,2} = -\left[(\gamma_\perp + \mathrm{i}\delta) \pm \mathrm{i}\Delta\omega\right]P_j^q - \mathrm{i}\frac{\mu^2}{\hbar}\left(E_1 W_{j1}^q \mathrm{e}^{\phi_+} + E_2 W_{j2}^q \mathrm{e}^{\phi_-}\right), \tag{8}$$

$$\begin{aligned}\frac{\mathrm{d}}{\mathrm{d}t}W_{ij}^{q=1,2} &= \gamma_\parallel R_{ij}^2 - \left(\gamma_\parallel \pm \mathrm{i}\Delta\omega\right)W_{ij}^q \\ &- \frac{\mathrm{i}}{4\hbar}\left[E_1^*\left(\alpha_{ij}^{11}P_1^q + \alpha_{ij}^{12}P_2^q\right)\mathrm{e}^{\phi_-} + E_2^*\left(\alpha_{ij}^{21}P_1^q + \alpha_{ij}^{22}P_2^q\right)\mathrm{e}^{\phi_+}\right] \\ &+ \frac{\mathrm{i}}{4\hbar}\left[E_1\left(\alpha_{ij}^{11}P_1^{(\overline{q}=2,1)*} + \alpha_{ij}^{21}P_2^{\overline{q}*}\right)\mathrm{e}^{\phi_+} + E_2\left(\alpha_{ij}^{12}P_1^{\overline{q}*} + \alpha_{ij}^{22}P_2^{\overline{q}*}\right)\mathrm{e}^{\phi_-}\right].\end{aligned} \tag{9}$$

2.2. Adiabatic polarization elimination (class-B laser equations)

If the radiative decay $\gamma_\perp$ is much faster than both the non-radiative decay $\gamma_\parallel$ and the eigenmode decay $\kappa_{1,2}$ (class-B lasers[18]), then the resulting equation system can be further simplified by assuming that polarization follows the field adiabatically, i.e., that $\mathrm{d}P_j^q(t)/\mathrm{d}t \approx 0$. After some algebra, Eqs. (7)–(9) are transformed to

$$\begin{aligned}\frac{\mathrm{d}}{\mathrm{d}t}E_1 &= -\frac{\kappa_1}{2}E_1 + \frac{\mu^2}{2\epsilon_0\epsilon\hbar}\frac{\omega_1}{\beta_1}\left(E_1 W_{11}^1\mathrm{e}^{\phi_+} + E_2 W_{12}^1\mathrm{e}^{\phi_-}\right), \\ \frac{\mathrm{d}}{\mathrm{d}t}E_2 &= -\frac{\kappa_2}{2}E_2 + \frac{\mu^2}{2\epsilon_0\epsilon\hbar}\frac{\omega_2}{\beta_2}\left(E_1 W_{21}^2\mathrm{e}^{\phi_+} + E_2 W_{22}^2\mathrm{e}^{\phi_-}\right),\end{aligned} \tag{10}$$

$$
\begin{aligned}
\frac{\mathrm{d}}{\mathrm{d}t}W_{ij}^{q=1,2} &= \gamma_{\parallel}R_{ij}^{q} - \left(\gamma_{\parallel} \pm \mathrm{i}\Delta\omega\right) W_{ij}^{q} \\
&\quad -\frac{\mu^2}{4\hbar^2}\frac{1}{\beta_q}\Big[\left|E_1\right|^2\left(\alpha_{ij}^{11}W_{11}^{q}+\alpha_{ij}^{12}W_{21}^{q}\right)+E_1^{*}E_2\left(\alpha_{ij}^{11}W_{12}^{q}+\alpha_{ij}^{12}W_{22}^{q}\right)\mathrm{e}^{2\phi_-} \\
&\qquad + E_2^{*}E_1\left(\alpha_{ij}^{21}W_{11}^{q}+\alpha_{ij}^{22}W_{21}^{q}\right)\mathrm{e}^{2\phi_+}+\left|E_2\right|^2\left(\alpha_{ij}^{21}W_{12}^{q}+\alpha_{ij}^{22}W_{22}^{q}\right)\Big] \\
&\quad -\frac{\mu^2}{4\hbar^2}\frac{1}{\beta_{\bar{q}=2,1}^{*}}\Big[\left|E_1\right|^2\left(\alpha_{ij}^{11}W_{11}^{\bar{q}*}+\alpha_{ij}^{21}W_{21}^{\bar{q}*}\right)+E_1E_2^{*}\left(\alpha_{ij}^{11}W_{12}^{\bar{q}*}+\alpha_{ij}^{21}W_{22}^{\bar{q}*}\right)\mathrm{e}^{2\phi_+} \\
&\qquad + E_2E_1^{*}\left(\alpha_{ij}^{12}W_{11}^{\bar{q}*}+\alpha_{ij}^{22}W_{21}^{\bar{q}*}\right)\mathrm{e}^{2\phi_-}+\left|E_2\right|^2\left(\alpha_{ij}^{12}W_{12}^{\bar{q}*}+\alpha_{ij}^{22}W_{22}^{\bar{q}*}\right)\Big]
\end{aligned}
\tag{11}
$$

where $\beta_{1,2} \equiv (\gamma_\perp + \mathrm{i}\delta) \pm \mathrm{i}\Delta\omega$ and the components R_{ij}^{q} are related to R in the same way as W_{ij}^{q} to W [Eqs. (4) and (6)]. We assume constant R in the gain region, but the model allows incorporation of spatially and/or temporally varying pumping. More specific knowledge about the modes in question makes it possible to simplify the system (10)–(11) further. If the modes are identical in intensity in the gain region, one can show that $W_{ij}^{(1,2)*} = W_{ij}^{2,1}$. This causes Eqs. (11) to assume a simpler form (13):

$$
\left|u_1(\mathbf{r})\right|^2 = \left|u_2(\mathbf{r})\right|^2,\ \mathbf{r}\in G \qquad \Rightarrow \qquad \alpha_{jj}^{ii} = \alpha_{ij}^{ji} \equiv \alpha, \tag{12}
$$

$$
\begin{aligned}
\frac{\mathrm{d}}{\mathrm{d}t}W_{ij}^{q=1,2} &= \gamma_{\parallel}R_{ij}^{q} - \left(\gamma_{\parallel} \pm \mathrm{i}\Delta\omega\right) W_{ij}^{q} \\
&\quad -\frac{\mu^2}{4\hbar^2}\left(\frac{1}{\beta_q}+\frac{1}{\beta_{\bar{q}}^{*}}\right)\Big[\left|E_1\right|^2\left(\alpha_{ij}^{11}W_{11}^{q}+\alpha_{ij}^{12}W_{21}^{q}\right)+\left|E_2\right|^2\left(\alpha_{ij}^{21}W_{12}^{q}+\alpha_{ij}^{22}W_{22}^{q}\right)\Big] \\
&\quad -\frac{\mu^2}{4\hbar^2}\Bigg[\left(E_1^{*}E_2\frac{\mathrm{e}^{2\phi_-}}{\beta_q}+E_1E_2^{*}\frac{\mathrm{e}^{2\phi_+}}{\beta_{\bar{q}}^{*}}\right)\left(\alpha_{ij}^{11}W_{12}^{q}+\alpha_{ij}^{12}W_{22}^{q}\right) \\
&\quad +\left(E_1^{*}E_2\frac{\mathrm{e}^{2\phi_-}}{\beta_{\bar{q}}^{*}}+E_1E_2^{*}\frac{\mathrm{e}^{2\phi_+}}{\beta_q}\right)\left(\alpha_{ij}^{21}W_{11}^{q}+\alpha_{ij}^{22}W_{21}^{q}\right)\Bigg].
\end{aligned}
\tag{13}
$$

Furthermore, considering the case that the modes are orthogonal in the gain region (so that $R_{ij\neq i} = 0$), as well as that both modes are equally coupled to the gain ($\delta = 0$), one can show that the population inversion components are grouped according to the symmetry of their subscripts: $W_{ii}^{1} = W_{ii}^{2*} \equiv W_s$, $W_{ij\neq i}^{1} = W_{ij}^{2*} \equiv W_a$ ("s" and "a" standing for "symmetric" and "anti-symmetric"). Introducing new variables $\mathcal{N}_{s,a} \equiv W_{s,a}\mathrm{e}^{\phi_\pm}$, after some algebra we get:

$$
\begin{aligned}
\frac{\mathrm{d}}{\mathrm{d}t}E_1 &= -\frac{\kappa_1}{2}E_1 + \frac{g\omega_1}{2}\mathcal{L}\left[E_1\mathcal{N}_s + E_2\mathcal{N}_a\right], \\
\frac{\mathrm{d}}{\mathrm{d}t}E_2 &= -\frac{\kappa_2}{2}E_2 + \frac{g\omega_2}{2}\mathcal{L}^{*}\left[E_1\mathcal{N}_a^{*} + E_2\mathcal{N}_s^{*}\right],
\end{aligned}
\tag{14}
$$

$$
\begin{aligned}
\frac{\mathrm{d}}{\mathrm{d}t}\mathcal{N}_s &= \frac{\gamma_{\parallel}}{2}R - \gamma_{\parallel}\mathcal{N}_s - \xi\mathcal{L}\alpha\left[\mathcal{N}_s\left(\left|E_1\right|^2+\left|E_2\right|^2\right)+\mathcal{N}_a\left(E_1^{*}E_2+E_1E_2^{*}\mathrm{e}^{4\phi_+}\right)\right], \\
\frac{\mathrm{d}}{\mathrm{d}t}\mathcal{N}_a &= -\left(\gamma_{\parallel}+2\mathrm{i}\Delta\omega\right)\mathcal{N}_a - \xi\mathcal{L}\alpha\left[\mathcal{N}_a\left(\left|E_1\right|^2+\left|E_2\right|^2\right)+\mathcal{N}_s\left(E_1^{*}E_2\mathrm{e}^{4\phi_-}+E_1E_2^{*}\right)\right],
\end{aligned}
\tag{15}
$$

with $g \equiv \mu/(2\epsilon_0\epsilon\hbar)$, $\xi \equiv \mu^2/(4\hbar^2)$, $\mathcal{L} \equiv \beta_1^{-1} + (\beta_2^{*})^{-1}$.

The system (14)–(15) describes the effects pertaining to the interaction between two modes, namely the incoherent self- and cross-saturation (due to the spatial hole burning), as well as coherent effects like the nearly degenerate four-wave mixing (owing to the population pulsations). It resembles the two-mode competition equations[21] generalized to the pump levels well above the lasing threshold.

So far, we have been considering the laser model without spontaneously emitted photons or any other signal external sources. These can be included phenomenologically by adding an explicitly time-dependent term to the field: $E(\mathbf{r},t) \rightarrow E(\mathbf{r},t) + \mathcal{E}(\mathbf{r},t)$ or to the polarization (which is equivalent as the polarization has been eliminated adiabatically).[18] In the rotating-wave approximation, this additional term will contribute to the slowly varying envelopes $E_i(t)$ as:

$$
\mathcal{E}_{1,2}(t) = \int_{t-\tau}^{t}\mathrm{d}t'\mathrm{e}^{\mp\mathrm{i}\Delta\omega t'}\int_C \mathrm{d}^3\mathbf{r}\epsilon(\mathbf{r})u_{1,2}^{*}(\mathbf{r})\mathcal{E}(\mathbf{r},t') \tag{16}
$$

where the spatial integration is over the whole cavity and the coarse-graining time integration is over $\tau > \Delta\omega^{-1}$, intended to average out all processes faster than τ. Unless $\mathcal{E}_j(t)$ are large enough to cause non-negligible feedback through population inversion, one can simply keep Eqs. (15) unchanged and supplement Eqs. (14) with $\mathcal{E}_j(t)$. A Langevin delta-correlated random function can be used in place of $\mathcal{E}(\mathbf{r},t)$ to model the noise, or an explicit form of an external signal can be used to model injection locked lasers.[8] In the simplest case when the injected signal $f_j(t)$ is designed to primarily excite one of the modes of the resonator, a solution of the following equation for a driven oscillator can be used:

$$\frac{\mathrm{d}^2}{\mathrm{d}t^2}\mathcal{E}_j(t) + 2\kappa_j\frac{\mathrm{d}}{\mathrm{d}t}\mathcal{E}_j(t) + \omega_j^2\mathcal{E}_j(t) = f_j(t). \tag{17}$$

2.3. Class-A equations: near-neutrally coupled modes

Here we introduce a further approximation of class-A lasers ($\gamma_\parallel \gg \kappa$), which, although not quite valid for the system under study, is a very illustrative limiting case of Eqs. (14)–(15). Within these assumptions, the components $\mathcal{N}_s$ and $\mathcal{N}_a$ are also adiabatically following the field envelopes ($\mathrm{d}\mathcal{N}_{s,a}/\mathrm{d}t \approx 0$). One can then expand the algebraic equations resulting from Eqs. (15) in a perturbative series, so that, in the first two orders,

$$\begin{aligned} \mathcal{N}_a^{(0)} &= 0, \qquad \mathcal{N}_a^{(1)} = -\frac{\xi\mathcal{L}\alpha R/2}{\gamma_\parallel + 2\mathrm{i}\delta\omega}E_1E_2^*, \\ \mathcal{N}_s^{(0)} &= R/2, \qquad \mathcal{N}_s^{(1)} = \frac{R}{2} - \frac{\xi\mathcal{L}\alpha R/2}{\gamma_\parallel}\left(|E_1|^2 + |E_2|^2\right). \end{aligned} \tag{18}$$

The Eqs. (14) then become

$$\begin{aligned} \frac{\mathrm{d}}{\mathrm{d}t}E_1 &= \left(-\frac{\kappa_1}{2} + \frac{R}{2}\frac{g\omega_1}{2}\mathcal{L}\right)E_1 - \frac{R}{2}\frac{\xi\mathcal{L}\alpha}{\gamma_\parallel}\left(|E_1|^2 + |E_2|^2\right)E_1 - \frac{R}{2}\frac{\xi\mathcal{L}\alpha}{\gamma_\parallel + 2\mathrm{i}\delta\omega}|E_2|^2E_1, \\ \frac{\mathrm{d}}{\mathrm{d}t}E_2 &= \left(-\frac{\kappa_2}{2} + \frac{R}{2}\frac{g\omega_2}{2}\mathcal{L}^*\right)E_2 - \frac{R}{2}\frac{\xi\mathcal{L}^*\alpha}{\gamma_\parallel}\left(|E_1|^2 + |E_2|^2\right)E_2 - \frac{R}{2}\frac{\xi\mathcal{L}^*\alpha}{\gamma_\parallel - 2\mathrm{i}\delta\omega}|E_1|^2E_2. \end{aligned} \tag{19}$$

We see that the resulting Eqs. (19) have the form of the usual linearized two-mode competition equations[8,10]

$$\frac{\mathrm{d}}{\mathrm{d}t}E_1 = \left(\rho_1 - \theta_{11}|E_1|^2 - \theta_{12}|E_2|^2\right)E_1, \qquad \frac{\mathrm{d}}{\mathrm{d}t}E_2 = \left(\rho_2 - \theta_{21}|E_1|^2 - \theta_{22}|E_2|^2\right)E_2. \tag{20}$$

For each mode, the first term ρ_j accounts for the net unsaturated gain minus losses, and the subsequent terms θ_{ij} account for self- and cross-saturation. One can notice that if the rightmost terms in Eqs. (19) [appearing due to the component $\mathcal{N}_a^{(1)}$ and clearly associated with coherent mode interaction terms in Eqs. (15)] are neglected, the equations become symmetric, and the self- and cross-saturation coefficient coincide. This corresponds to the neutral coupling between the modes ($C \equiv \theta_{12}\theta_{21}/\theta_{11}\theta_{22} = 1$). The modes can lase stably in any proportion, provided the sum of their intensities remains the same. The inclusion of the omitted terms results in the mode coupling constant slightly exceeding unity:

$$C = 1 + 3\gamma_\parallel^2/\left(\gamma_\parallel^2 + 4\Delta\omega^2\right). \tag{21}$$

We see that even in this simplified case the system can exhibit mode coupling which is slightly stronger than neutral,[17] and the coherent mode interaction processes are likely to be causing such behavior. However, as $\gamma_\parallel \ll \Delta\omega$, the addition to C is extremely small, and it is expected that any deviation of the system from the ideal case [such as a slight perturbation of the mode intensity equality. (12)] will push the system back into the weak mode coupling regime.

3. MODE COMPETITION REGIMES AND BISTABILITY

As a model to demonstrate bistability, we have chosen a structure that closely fits the model developed, namely, a structure consisting of twin coupled defects in a 2D PhC square lattice (Fig. 1). The defects are assumed to be identical and contain a gain medium. The resulting resonator thus exhibits two modes arising from the splitting of the fundamental mode of a single defect. These two modes (see Fig. 1) are spectrally close to each other (the distance dependent on the coupling

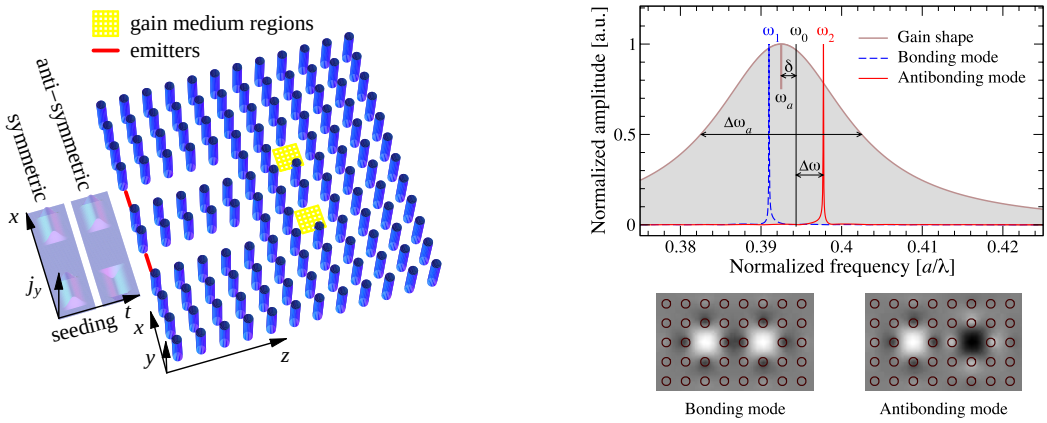

Figure 1. Twin coupled defects in a 2D PhC square lattice with period $a = 500$ nm along with the spectra and schematic field distribution of the system's eigenmodes. Also shown are sample pulsed signals [seeding $j_y(\mathbf{r}, t)$] than can selectively excite the desired mode with a matching phase structure [according to Eq. (17)]. The PhC waveguides adjacent to the defects can be used to deliver those signals, as well as to guide the output laser radiation out of the resonator.

strength between cavities), and if no losses are assumed in the coupling region, they have close Q-factors. Their primary difference is in the phase relations between the fields oscillating in each cavity: the lower-frequency "bonding" mode and the higher-frequency "antibonding" mode (the notation similar to that used for modes in photonic molecules[15]) have the field in the two cavities oscillating in phase and in antiphase, respectively. Note that this *phase* difference, which is what makes such modes individually excitable by a signal with the matching symmetry (as shown in Fig. 1, following an earlier suggestion[22]), does not influence the modes' *intensity* profile, which is nearly identical in the cavities (i.e., where there is the gain medium) and only differs in the coupling region. This makes the structure in question conform to the condition. (12) used to obtain Eqs. (14)–(15). This system of equations was solved numerically for the parameters corresponding to the structure in Fig. 1, the results compared with the finite-difference time-domain (FDTD) simulation of lasing in the same system (the reader is referred to our earlier paper[9] for further details).

Let us begin by analyzing the mode dynamics as dependent on the pumping rate (Fig. 2). Moderate pumping levels cause the overall mode dynamics to exhibit the known spiking behavior (Fig. 2a), which disappears when the laser is operated well above the threshold (Fig. 2b,c). As regards the mode interaction, we see that there is a clear transition from a slow convergence towards simultaneous two-mode lasing (Fig. 2a,b), to the case when the weaker mode is quenched by (instead of catching up with) the stronger mode. By the stronger mode we mean the one which happens to have an advantage at the period of lasing onset. Hence, either mode that has an initial advantage can become dominant in lasing (Fig. 2c,d), which is a direct indication of bistable two-mode lasing.

This transition from two-mode to bistable lasing can be explained by qualitative analytical considerations. Let us suppose that one mode lases in a stationary state: $E_1(t) = 0$, $E_2(t) = E$, from Eqs. (15) it follows that $\mathcal{N}_s(t) = \eta E$, $\mathcal{N}_a(t) = 0$. Suppose that a slight perturbation is present, so that

$$E_1 \to \delta E, \quad E_2 \to E - \delta E, \quad \mathcal{N}_a \to \delta\mathcal{N}. \tag{22}$$

Such perturbation, while keeping $\mathcal{N}_s$ unperturbed, assures that only the balance between the modes is shifted but not the overall lasing intensity $|E_1|^2 + |E_2|^2$, so that its dynamics, which is always stable above the lasing threshold, does not obscure the mode interaction dynamics, which we are trying to investigate. The equations for small variations are:

$$\begin{aligned} \frac{\mathrm{d}}{\mathrm{d}t}\delta E &= -\frac{\kappa}{2}\delta E + g\frac{\omega}{2}\mathcal{L}\left(\eta E\delta E + E\delta\mathcal{N}\right), \\ \frac{\mathrm{d}}{\mathrm{d}t}\delta\mathcal{N} &= -\left(\gamma_{\parallel} + 2\mathrm{i}\Delta\omega\right)\delta\mathcal{N} - \xi\alpha\mathcal{L}\left(|E|^2\,\delta\mathcal{N} + \eta E E^*\delta E\right). \end{aligned} \tag{23}$$

Assuming that both δE and $\delta\mathcal{N}$ are varying as e^{st}, and that $\delta\mathcal{N} = \eta\delta E$, we write the secular equation[8] for s

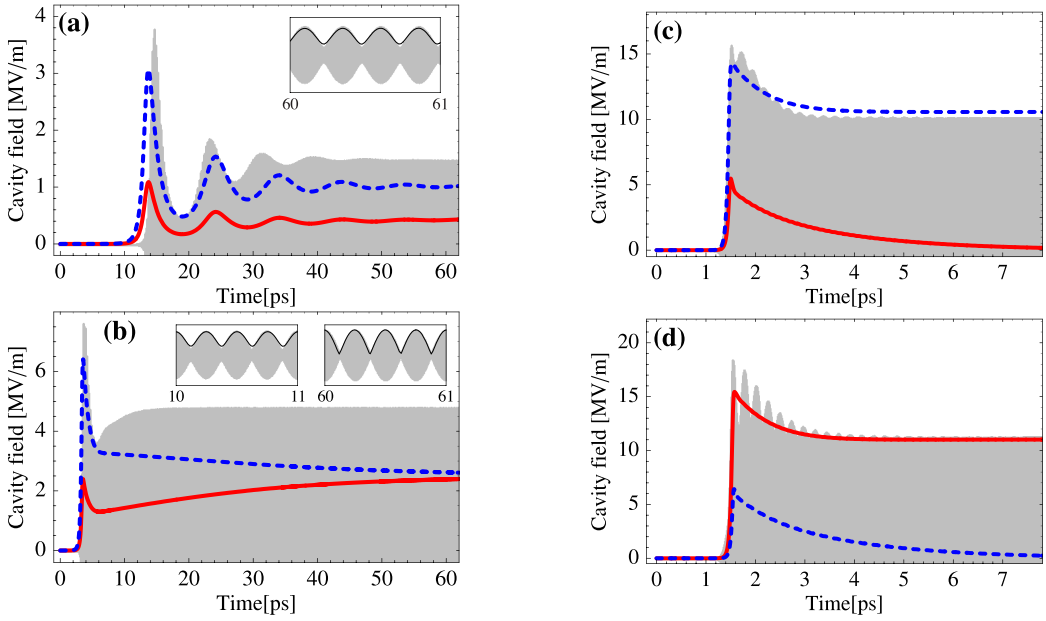

Figure 2. The evolution of the mode amplitudes $|E_1(t)|$ and $|E_2(t)|$ (solid and dashed line, respectively), normalized to the units of cavity field, for **(a)** $R = 10^8$; **(b)** $R = 10^9$; **(c, d)** $R = 10^{10}$ (in arbitrary units). The shaded graph shows the cavity field as obtained by FDTD calculations for comparison. The insets show time-resolved intermode beatings in FDTD cavity field (shaded) and in the cavity field reconstructed from $|E_j(t)|$ (solid). The modes were initially excited with proportion $\mathcal{E}_1 : \mathcal{E}_2$ equal to **(a, b, c)** $1 : 3$ and **(d)** $3 : 1$.

$$\begin{vmatrix} s + \kappa/2 - g(\omega/2)\mathcal{L}\eta E & -g(\omega/2)\eta E \\ \xi\alpha\mathcal{L}\,|E|^2 & s + \left(\gamma_{\parallel} + 2\mathrm{i}\Delta\omega\right) + \xi\alpha\mathcal{L}\,|E|^2 \end{vmatrix} = 0. \tag{24}$$

The resulting quadratic equation for s has two characteristic cases: for smaller R, there can be solutions with $\mathrm{Re}\, s > 0$, suggesting that one-mode lasing can be unstable. When R is increased, it can be shown that $\mathrm{Re}\ s < 0$, which means that one-mode lasing regime is stable. This marks the transition from simultaneous to bistable lasing. Inserting the parameters for the model system in Fig. 1 into Eq. 24, one obtains the critical value of R to be between 10^9 and 10^{10}, consistent with the observations in Fig. 2.

The limiting case dealt with in Sec. 2.3 has shown that in the lower orders of expansion $\mathcal{N}_s$ and $\mathcal{N}_a$ correspond to incoherent (hole-burning) and coherent (population-pulsation) mode interaction processes, respectively. It has also been shown that hole burning alone cannot bring the mode coupling constant past unity. This is intuitively clear: when two modes coexist in the same resonator and have the same intensity in the same volume (as is our case), the incoherent, intensity-related effects will not discriminate between these two modes, and each mode will equally be saturating both itself and its counterpart, which is exactly the case of neutral mode coupling. In any real resonator, the intensity distribution equality (12) is expected to be perturbed even without taking into account the adverse effects of material or fabrication imperfection losses. So each mode is likely to interact with its counterpart slightly weaker than with itself, making neutral coupling, let alone bistability, unattainable in coupled cavity based design by merely incoherent mode interaction.

On the contrary, population pulsation assisted coherent mode interaction is capable of taking into account the phase structure of the modes in question. Hence, it is the coherent mode interaction that can bring the cross-saturation between modes past the self-saturation. On the other hand, the near-identical intensity distribution (12) within the gain medium takes care that spatial hole burning brings the mode coupling as close to neutral as possible. So, an interplay between coherent and incoherent mode interaction processes is the cause of bistability in coupled-cavity laser resonators. It remains an open question whether such “constructive” interplay is a general property of coupled cavities, and what cavity parameters are responsible for achieving the optimum in that interplay. This is a promising subject of future investigations.

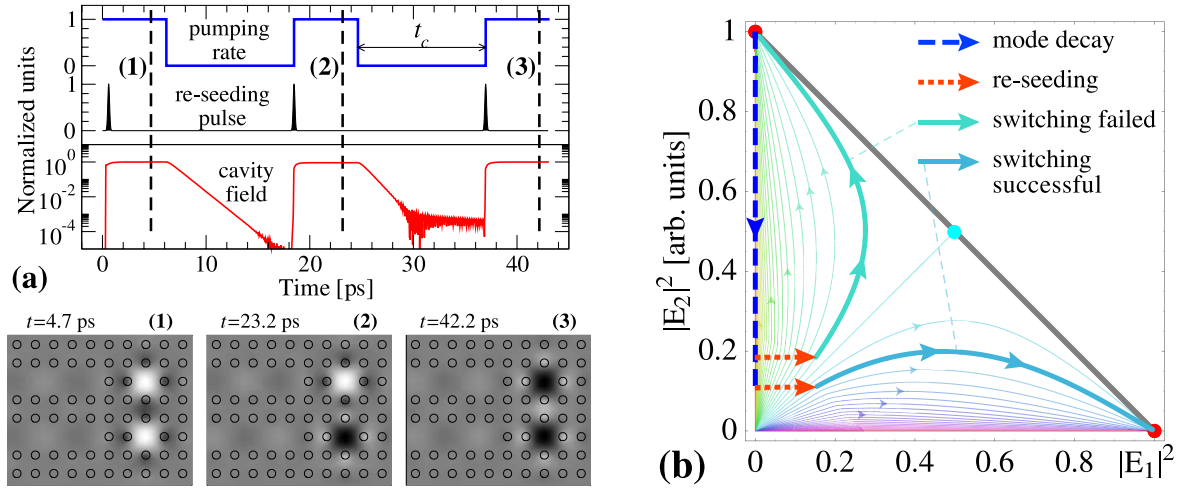

Figure 3. (a) The time diagram of numerical simulation for $1 \to 2 \to 1$ mode switching, the insets showing the spatial distribution of cavity field in the steady-state lasing regime.[17] **(b)** The schematic phase diagram of bistable laser described by Eqs. (14)–(15), with illustration of successful and unsuccessful $2 \to 1$ mode switching (see text for details).

4. MODE SWITCHING DYNAMICS

Having established that bistability is possible in coupled cavity based microlasers, we proceed to investigate the operating dynamics of the proposed laser in a mode-to-mode switching regime. The idea of mode switching proposed earlier[17] consists of two phases. First, the pumping is turned off for a certain time t_c; secondly, the laser is re-seeded (i.e., locked into a different mode) simultaneously with turning the pumping back on. As shown in earlier numerical simulations, switching between the two modes is indeed possible on a picosecond time scale (Fig. 3a). Using the theory presented in previous sections, we can analyze the dynamics of the switching process further.

Figure 3b schematically depicts the phase diagram of the laser, using the normalized mode amplitudes $|E_{1,2}|^2$ as phase variables. Any state of the laser corresponds to a point, the temporal evolution represented by phase trajectory lines. Since the system is bistable, the phase trajectories converge towards one of the two stable fixed points of single-mode lasing: $(0;1)$ or $(1;0)$, depending on the initial state of the resonator, brought into the equations (14)–(15) by the pulsed locking (called *seeding*[8]) via non-homogeneous terms (16). The line between the origin and the unstable fixed point $(0.5;0.5)$ divides the space into two domains. In each of them, all points find themselves on trajectories that converge to the stable fixed point lying in that domain. Hence, giving one mode an advantage at the onset of lasing corresponds to placing the resonator into the corresponding domain. One can see in Figs. 2–**??** that the shape of phase trajectories should depend on R, but the idea is not changed as long as R is large enough to achieve bistability.

As soon as the pumping is turned off ($R = 0$), the phase diagram is drastically altered. Only the origin $(0;0)$ remains as a stable fixed point, and if $\kappa_1 \approx \kappa_2$, the phase trajectories are straight lines converging there. This corresponds to the exponential mode decay with rates κ_j [see, e.g., Eq. (19)] from the steady-state amplitude $\left|E_j^{\text{sat}}\right|^2$ towards the origin, described as

$$E_j(t) = E_j^{\text{sat}} \exp\left[-\left(\kappa_j/2\right) t\right], \tag{25}$$

shown as a dashed line in Fig. 3b. The signal that is supposed to lock the laser into the other mode by giving it a "boost" can be schematically represented by shifting the resonator state on the phase diagram perpendicularly to the decay trajectory (dotted line). If the pumping is turned on immediately afterwards, the system will follow the lines of the phase diagram for a system with gain. The critical factor in the further system evolution is whether the re-seeding has succeeded to shift the resonator state past the dividing line into the other mode's domain. If this is the case, switching is seen to occur. If not, e.g., if re-seeding occurred prematurely and the resonator remains in the same domain, then lasing simply resumes at the original mode (see Fig. 3b). As a result, there is a simple relation between the minimum decay time t_c^{min}, the relative amplitude of re-seeding signal $\varepsilon_i \equiv \mathcal{E}_i / E_j^{\text{sat}}$, and the mode decay rates κ_j for $j \to i$ mode switching:

$$\varepsilon_i = \exp\left[-\left(\kappa_j/2\right) t_c^{\text{min}}\right]. \tag{26}$$

This relations is in agreement with earlier numerical predictions.[17] The phase diagram approach allows to analyze the effect of mode switching in more detail, e.g., taking into account the finite duration of the re-seeding signal, as well as to consider the effects resulting from temporal mismatch between re-seeding and turning the pumping on.

5. CONCLUSIONS

We have shown that bistable lasing is possible in a coupled cavity based microresonator without the need for a saturable absorber[14] or very low Q-factor.[11–13] By expanding the earlier theory[18] to the case of two modes of arbitrary geometrical structure, we have shown that bistability is the result of an interplay between incoherent and coherent mode interaction. Incoherent effects alone cannot bring the modes coexisting in a cavity to stronger-than-neutral coupling. Further extension of the formalism developed, e.g., to include spatial as well as temporal multiscale analysis,[20] will allow to extend the conclusions of the present paper not only to defect-based, but also to distributed feedback based microlasers.

The reported bistability is a prerequisite to a new principle in multiple-wavelength microlaser design based on deliberate mode selection by locking into the chosen mode in a multimode resonator[9,17] rather than externally tuning the entire cavity.[5–7] Analytical predictions agree with FDTD numerical simulation of lasing in twin coupled defects in a 2D photonic crystal lattice.[17] Contrary to earlier accounts,[15,16] both coupled cavities are identical, which makes the intermodal frequency splitting controllable, e.g., by varying the inter-cavity distance, and even tunable by conventional means.[5] The mode switching dynamics has been studied in detail using the theoretical analysis developed. The tolerance of the switchable lasing to the adverse effects of fabricational imperfections remains an interesting subject of future investigations.

ACKNOWLEDGMENTS

The authors thank the Deutsche Forschungsgemeinschaft for financial support (Projects SPP 1113 and FOR 557). One of us (AVL) wishes to acknowledge the Danish Technical Research Council via PIPE project and the EU Commission FP6 via project NewTon (NMP4-CT-2005-017160).

REFERENCES

1. M. Imada, A. Chutinan, S. Noda, and M. Mochizuki, "Multidirectionally distributed feedback photonic crystal lasers", *Phys. Rev. B* **65**, 195306, 2002; O. Painter, R. K. Lee, A. Scherer, A. Yariv, D. O'Brien, P. D. Dapkus, and I. Kim, "Two-dimensional photonic band-gap defect mode laser," *Science* **284**, pp. 1819–1821, 1999.
2. J. C. Johnson, H. Q. Yan, R. D. Schaller, L. H. Haber, R. J. Saykally, and P. D. Yang, "Single Nanowire Lasers," J. Phys. Chem. B **105**, pp. 11387–11390, 2001.
3. M. Fujita, R. Ushigome, and T. Baba, "Continuous wave lasing in GaInAsP microdisk injection laser with threshold current of $40\ \mu$A", *Electron. Lett.* **27**, pp. 790–791, 2000;
4. H.-Y. Ryu, C.-H. Kwon, Y.-J. Lee, Y.-H. Lee, and J.-S. Kim, "Very-low-threshold photonic band-edge lasers from free-standing triangular photonic crystal slabs", *Appl. Phys. Lett.* **80**, pp. 3476–3478, 2002.
5. W. Park and J.-B. Lee, "Mechanically tunable photonic crystal structure", *Appl. Phys. Lett.* **85**, pp. 4845–4847, 2004.
6. H. Yu, B. Tang, J. Li, and Le Li, "Electrically tunable lasers made from electro-optically active photonics band gap materials", *Opt. Express* **13**, pp. 7243–7249, 2005;
7. E. P. Kosmidou, E. E. Kriezis, and T. D. Tsiboukis, "Analysis of tunable photonic crystal devices comprising liquid crystal materials as defects", *IEEE J. Quant. Electron.* **41**, pp. 657–665, 2005.
8. A. Siegman, *Lasers* (University Science Books, Mill Valley, CA, 1986).
9. S. V. Zhukovsky, D. N. Chigrin, A. V. Lavrinenko, and J. Kroha, "Selective lasing in multimode periodic and non-periodic nanopillar waveguides", *Phys. Stat. Sol. b* **244**, pp. 1211–1218, 2007.
10. M. Sargeant III, M. O. Scully, and W. E. Lamb, Jr., *Laser Physics* (Addison-Wesley, Reading, MA, 1974).
11. J. L. Oudar and R. Kuszelewicz, "Demonstration of optical bistability with intensity-coupled high gain lasers," *Appl. Phys. Lett.* **45**, pp. 831–833, 1984;
12. R. Kuszelewicz and J. L. Oudar, "Theoretical analysis of a new class of optical bistability due to non-coherent coupling within a twin-laser system", *IEEE J. Quant. Electron.* **QE-23**, pp. 411–417, 1987.
13. J. L. Oudar and R. Kuszelewicz, "Bistabilité optique des lasers couplés, *Revue Phys. Appl.* **22**, pp. 1287–1295, 1987.

14. C. L. Tang, A. Schremer, and T. Fujita, "Stability in two-mode semiconductor lasers via gain saturation", *Appl. Phys. Lett.* **51**, pp. 1392-1394, 1987; C.-F. Lin and P.-C. Ku, "Analysis of stability in two-mode laser systems", *IEEE J. Quant. Electron.* **32**, pp. 1377–1382, 1996.
15. S. Ishii and T. Baba, "Bistable lasing in twin microdisk photonic molecues", *Appl. Phys. Lett.* **87**, 181102, 2005.
16. M. Hill, H. Dorren, T. de Vries, X. Leijtens, J. Hendrik den Besten, B. Smalbrugge, Y.-S. Oei, H. Binsma, G.-D. Khoe, and M. Smit, "A fast low-power optical memory based on coupled micro-ring lasers", *Nature* **432**, pp. 206–209, 2004.
17. S. V. Zhukovsky, D. N. Chigrin, A. V. Lavrinenko, and J. Kroha, "Switchable lasing in coupled multimode microcavities", arXiv:cond-mat/0701619 (unpublished).
18. S. E. Hodges, M. Munroe, J. Cooper, and M. G. Raymer, "Multimode laser model with coupled cavities and quantum noise," *J. Opt. Soc. Am. B* **14**, pp. 191–197, 1997.
19. K. Otsuka, P. Mandel, S. Bielawski, D. Derozier, and P. Glorieux, "Alternate time scale in multimode lasing", *Phys. Rev. A* **46**, pp. 1692–1696, 1992.
20. L. Florescu, K. Busch, and S. John, "Semiclassical theory of lasing in photonic crystals," *J. Opt. Soc. Am. B* **19**, pp. 2215–2223, 2002.
21. K. Staliunas, M. F. H. Tarroja, and C. O. Weiss, "Transverse mode locking, antilocking and self-induced dynamics of class-B lasers", *Opt. Commun.* **102**, pp. 69–75, 1993.
22. D. N. Chigrin, A. V. Lavrinenko, and C. M. Sotomayor Torres, "Nanopillar photonic crystal waveguides," *Opt. Express* **12**, pp. 617–622, 2004.